PHYSICAL REVIEW E **95**, 062804 (2017)

Effect of impurities on chirality conversion by grinding

Hiroyasu Katsuno[1,*] and Makio Uwaha[2,†]
[1]*Department of Physical Sciences, Ritsumeikan University, 1-1-1 Nojihigashi, Kusatsu, Shiga 525-8577, Japan*
[2]*Science Division, Center for General Education, Aichi Institute of Technology, 1247 Yachigusa, Yakusa-cho, Toyota, Aichi 470-0392, Japan*

(Received 11 April 2017; published 30 June 2017)

We study the effect of chiral impurities on Viedma ripening using a simple reaction model. The exponential amplification of the enantiomeric excess (EE) is greatly accelerated by a smaller growth rate of solids with monomers caused by the chiral impurities. From the analysis of the model, it is found that the time evolution of the EE is essentially described by a second-order differential equation. The effect of chiral impurities is that the unstable fixed point is shifted from the racemic point, which leads to the linear amplification behavior observed experimentally. The analysis also shows a possibility of an oscillatory decay of the EE.

DOI: 10.1103/PhysRevE.95.062804

I. INTRODUCTION

Spontaneous chiral symmetry breaking of sodium chlorate ($NaClO_3$) crystallization was found by Kondepudi *et al.* [1–3]. $NaClO_3$ crystals were made from a supersaturated solution with stirring, and almost all crystals grown from the solution in each experiment has the same chirality, which is completely random. The cause of this phenomenon is attributed to secondary nucleation [2–8]. A large nucleus is broken into pieces by stirring, and generated small nuclei which work as crystal seeds in the solution. In 2005, Viedma demonstrated the complete chiral resolution of $NaClO_3$ crystals (which is called Viedma ripening) in which secondary nucleation is irrelevant [9]. Chiral crystals of both chirality are put in a saturated solution with glass beads and the solution is stirred. Crystals are ground by the glass beads, and the enantiomeric excess (EE) is amplified exponentially with time. At the end, all crystals have the same chirality, that is, the other type of crystals initially present disappear. The minority type crystals are converted to the majority type.

After the discovery of Viedma ripening, similar phenomena have been found for various organic molecules [10,11]. By stirring a solution with crystals and glass beads, a small initial EE of solids in a solution can be amplified and enantiopure crystals are obtained. Making enantiopure crystals is important in chemical engineering, and finding the mechanism is interesting from the viewpoint of physics and chemistry. It is arguable what kind of kinetic growth processes are important. To explain Viedma ripening, several theoretical models have been proposed such as cluster incorporation [12–24], surface reaction [25], and mutual inhibition [26,27]. These models, which are based on an autocatalytic reaction and a recycling process [3,28], can reproduce the exponential amplification of EE observed in experiment.

Noorduin *et al.* [29] reported a complete chiral resolution of amino acid crystals by Viedma ripening with chiral additives. They pointed out that the chirality of prevailing crystals is the opposite to that of the additive. Steendam *et al.* [24] have also performed a similar experiment and observed a linear amplification of the EE with chiral additives. Using a rate equation model with the cluster incorporation mechanism [14], the linear amplification of the EE is reproduced by a change of the reaction rate due to chiral additives [24]. However, it is difficult to connect their conclusion to the case without chiral impurities because their assumption that the masses of crystals change linearly in time during the EE amplification cannot be applied.

In this paper, we study in detail the effect of chiral impurities on the EE amplification using a simple rate equation model similar to that of Ref. [24]. Our purpose is to specify (i) which kinetic process is important on the EE amplification, and (ii) what causes the change from the exponential amplification to the linear amplification by adding chiral impurities. In Sec. II, our rate equation model is introduced. From numerical results, we obtain the apparent linear amplification of the EE in certain cases and specify the key process of the EE amplification in Sec. III. We will show that the unstable fixed point of the exponential amplification of the EE in a phase space is shifted from the racemic state when chiral impurities suppress the reaction rate. This is the origin of the linear amplification. We summarized our results in Sec. IV.

II. RATE EQUATION ANALYSIS

In the grinding experiments [9–11], crystals are ground by stirring a solution with glass beads. The simple reaction model can reproduce the behavior of the exponential amplification of the EE [12]. The system is uniform and the size distribution of crystals does not seem to be crucial. Steendam *et al.* [24] have shown the effect of chiral impurities experimentally and theoretically for an organic system. Using a six-component system (two chiral molecules, two chiral clusters, and two chiral solids) based on the simple reaction model [14], they studied the effect of impurities. If the reaction rates between monomers and solids, and those between monomers and clusters for one chiral species are suppressed by chiral impurities, the linear amplification of the EE appears.

In this paper, the effect of chiral impurities on the EE amplification is studied again using a simplified rate equation model based on Ref. [24]. Since Steendam *et al.* found that the behavior of the EE amplification is not sensitive to the racemization rate of molecules when the racemization rate is fast enough, we take the limit of fast racemization. Our model has masses of the five components: achiral molecules Z in a

---

[*] katsuno@fc.ritsumei.ac.jp
[†] uwaha@nagoya-u.jp

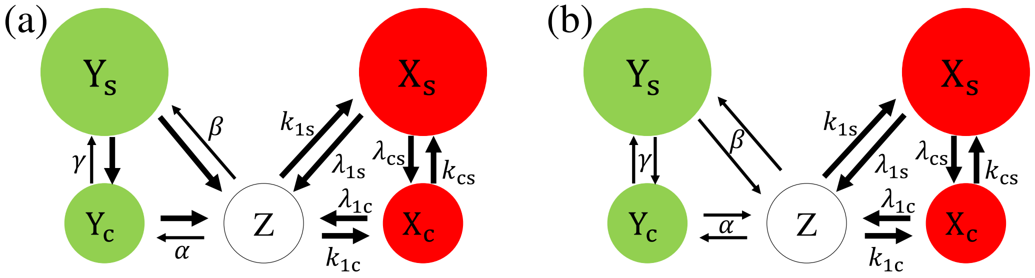

FIG. 1. Schematic view of the reaction processes of (a) type I impurities and (b) type II impurities.

solution, a pair of chiral clusters $\mathrm{X_c}$ and $\mathrm{Y_c}$, and a pair of chiral solids $\mathrm{X_s}$ and $\mathrm{Y_s}$. The system also corresponds to the inorganic system such as $\mathrm{NaClO_3}$.

Two types of chiral impurities are considered. The first type changes the equilibrium balance of each component (type I), and the second one does not change the equilibrium balance but the growth and dissolution rates (type II). In the first case, the enantiopure state can be achieved without the cluster reaction [30]. The special case of the second type is studied in Ref. [24]. Here, we study the simple reaction model in more detail to find the kinetic process crucial to the chirality conversion.

We describe the system with the relative ratio of masses: z, $x_{\rm c}$, $y_{\rm c}$, $x_{\rm s}$, and $y_{\rm s}$. They are the normalized masses of the monomers Z, the chiral clusters $\mathrm{X_c}, \mathrm{Y_c}$, and the chiral solids $\mathrm{X_s}, \mathrm{Y_s}$, respectively. The total mass is conserved: $z + x_{\rm c} + y_{\rm c} + x_{\rm s} + y_{\rm s} = 1$. The monomers and the chiral clusters are the growth units in our system as shown in Figs. 1(a) and 1(b). Here, we introduce two types of impurities to the simple reaction model, whose reactions are summarized in Table I. Type I impurities make the growth rate of Y crystals smaller with reduction factors $\alpha_{\rm I}$, $\beta_{\rm I}$, and $\gamma_{\rm I}$:

$$\dot{z} = -(k_{1\rm c}z - \lambda_{1\rm c})x_{\rm c} - (\alpha_{\rm I}k_{1\rm c}z - \lambda_{1\rm c})y_{\rm c} - (k_{1\rm s}z - \lambda_{1\rm s})x_{\rm s} - (\beta_{\rm I}k_{1\rm s}z - \lambda_{1\rm s})y_{\rm s}, \tag{1}$$

$$\dot{x}_c = (k_{1\rm c}z - \lambda_{1\rm c})x_{\rm c} - (k_{\rm cs}x_{\rm c} - \lambda_{\rm cs})x_{\rm s}, \tag{2}$$

$$\dot{y}_c = (\alpha_{\rm I}k_{1\rm c}z - \lambda_{1\rm c})y_{\rm c} - (\gamma_{\rm I}k_{\rm cs}y_{\rm c} - \lambda_{\rm cs})y_{\rm s}, \tag{3}$$

TABLE I. All reactions in Fig. 1.

Type I	Type II
$\mathrm{Z + X_c} \underset{k_{1\rm c}}{\overset{\lambda_{1\rm c}}{\leftrightharpoons}} \mathrm{X_c}$	$\mathrm{Z + X_c} \underset{k_{1c}}{\overset{\lambda_{1\rm c}}{\leftrightharpoons}} \mathrm{X_c}$
$\mathrm{Z + Y_c} \underset{\alpha k_{1\rm c}}{\overset{\lambda_{1\rm c}}{\leftrightharpoons}} \mathrm{Y_c}$	$\mathrm{Z + Y_c} \underset{\alpha k_{1\rm c}}{\overset{\alpha\lambda_{1\rm c}}{\leftrightharpoons}} \mathrm{Y_c}$
$\mathrm{Z + X_s} \underset{k_{1\rm s}}{\overset{\lambda_{1\rm s}}{\leftrightharpoons}} \mathrm{X_s}$	$\mathrm{Z + X_s} \underset{k_{1\rm s}}{\overset{\lambda_{1\rm s}}{\leftrightharpoons}} \mathrm{X_s}$
$\mathrm{Z + Y_s} \underset{\beta k_{1\rm s}}{\overset{\lambda_{1\rm s}}{\leftrightharpoons}} \mathrm{Y_s}$	$\mathrm{Z + Y_s} \underset{\beta k_{1\rm s}}{\overset{\beta\lambda_{1\rm s}}{\leftrightharpoons}} \mathrm{Y_s}$
$\mathrm{X_c + X_s} \underset{k_{\rm cs}}{\overset{\lambda_{\rm cs}}{\leftrightharpoons}} \mathrm{X_s}$	$\mathrm{X_c + X_s} \underset{k_{\rm cs}}{\overset{\lambda_{\rm cs}}{\leftrightharpoons}} \mathrm{X_s}$
$\mathrm{Y_c + Y_s} \underset{\gamma k_{\rm cs}}{\overset{\lambda_{\rm cs}}{\leftrightharpoons}} \mathrm{X_s}$	$\mathrm{Y_c + Y_s} \underset{\gamma k_{\rm cs}}{\overset{\gamma\lambda_{\rm cs}}{\leftrightharpoons}} \mathrm{Y_s}$

$$\dot{x}_s = (k_{1\rm s}z - \lambda_{1\rm s})x_{\rm s} + (k_{\rm cs}x_{\rm c} - \lambda_{\rm cs})x_{\rm s}, \tag{4}$$

$$\dot{y}_s = (\beta_{\rm I}k_{1\rm s}z - \lambda_{1\rm s})y_{\rm s} + (\gamma_{\rm I}k_{\rm cs}y_{\rm c} - \lambda_{\rm cs})y_{\rm s}. \tag{5}$$

Type II impurities make the growth and dissolution rates of Y crystals smaller with the same ratio $\alpha_{\rm II}$, $\beta_{\rm II}$, and $\gamma_{\rm II}$:

$$\dot{z} = -(k_{1\rm c}z - \lambda_{1\rm c})x_{\rm c} - \alpha_{\rm II}(k_{1\rm c}z - \lambda_{1\rm c})y_{\rm c} - (k_{1\rm s}z - \lambda_{1\rm s})x_{\rm s} - \beta_{\rm II}(k_{1\rm s}z - \lambda_{1\rm s})y_{\rm s}, \tag{6}$$

$$\dot{x}_c = (k_{1\rm c}z - \lambda_{1\rm c})x_{\rm c} - (k_{\rm cs}x_{\rm c} - \lambda_{\rm cs})x_{\rm s}, \tag{7}$$

$$\dot{y}_c = \alpha_{\rm II}(k_{1\rm c}z - \lambda_{1\rm c})y_{\rm c} - \gamma_{\rm II}(k_{\rm cs}y_{\rm c} - \lambda_{\rm cs})y_{\rm s}, \tag{8}$$

$$\dot{x}_s = (k_{1\rm s}z - \lambda_{1\rm s})x_{\rm s} + (k_{\rm cs}x_{\rm c} - \lambda_{\rm cs})x_{\rm s}, \tag{9}$$

$$\dot{y}_s = \beta_{\rm II}(k_{1\rm s}z - \lambda_{1\rm s})y_{\rm s} + \gamma_{\rm II}(k_{\rm cs}y_{\rm c} - \lambda_{\rm cs})y_{\rm s}. \tag{10}$$

The terms with $k_{1\rm c}$ and $k_{1\rm s}$ represent the growth of chiral clusters and chiral solids with monomers. The terms with $k_{\rm cs}$ represent the growth of chiral solids with chiral clusters. The terms with $\lambda_{1\rm c}$ and $\lambda_{1\rm s}$ represent decay of chiral clusters and chiral solids by detachment of monomers. The terms with $\lambda_{\rm cs}$ represent decay of chiral solids by detachment of chiral clusters. The coefficients α, β, and γ represent the reduction ratios of the related rates by the chiral impurities. When $\alpha_{\rm II} = \beta_{\rm II}$ and $\gamma_{\rm II} = 1$, the system is the same as the fast racemization limit of Ref. [24]. The values of parameters we use in the numerical calculation are $k_{1\rm c} = 0.1$, $k_{1\rm s} = k_{\rm cs} = 1$, $\lambda_{1\rm c} = 0.05$, $\lambda_{1\rm s} = \lambda_{\rm cs} = 0.1$ [31]. The initial values of the relative masses are $z = 0.1$, $x_{\rm c} = y_{\rm c} = 0.05$, $x_{\rm s} = 0.44$, and $y_{\rm s} = 0.36$.

III. RESULTS AND INTERPRETATION

Figure 2 shows the time change of the EE of solids $\phi_{\rm s}$ defined by $\phi_{\rm s} = (x_{\rm s} - y_{\rm s})/(x_{\rm s} + y_{\rm s})$ for the initial EE $\phi_{\rm s}(0) = 0.1$. With type I impurities, the amplification of the EE is accelerated in all cases we tried as shown in Fig. 2(a). When the growth rate between monomers and clusters is reduced, the effect of the reduction parameter α on the EE amplification is rather small (green). When the growth rate between monomers and solids (blue) or that between clusters and solids (magenta) is reduced, clear acceleration is visible. In particular, in the case of the reduction of the growth rate between monomers and solids, the linear amplification is seen. With type II impurities, when the rate between monomers and clusters or that between clusters and solids is suppressed [green or magenta in Fig. 2(b)], the EE becomes negative, and the initial minority crystals $\mathrm{Y_s}$ dominate. When the rate between monomers and solids is suppressed, the amplification of the

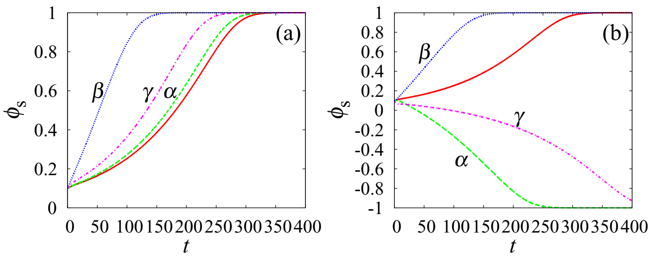

FIG. 2. Time dependence of ϕ_{s} with (a) type I impurities for $(\alpha_{\mathrm{I}},\beta_{\mathrm{I}},\gamma_{\mathrm{I}}) = (0.9,1,1)$ (green dashed), $(1,0.9,1)$ (blue dotted), and $(1,1,0.9)$ (magenta dash-dotted), and (b) type II impurities for $(\alpha_{\mathrm{II}},\beta_{\mathrm{II}},\gamma_{\mathrm{II}}) = (0.25,1,1)$ (green dashed), $(1,0.25,1)$ (blue dotted), and $(1,1,0.25)$ (magenta dash-dotted). The red solid line in both figures shows the EE without impurities.

EE is accelerated and the linear amplification is seen (blue). The effect of type I impurities is simple, and that of type II impurities seems to have some complexity.

We study the time development of the EE as seen in Fig. 2 in detail. Without grinding, a stable steady state with $x_{\mathrm{s}} = y_{\mathrm{s}} \neq 0$ is interpreted as the stable racemic state where the EE is 0. From previous studies such as Refs. [12,28], in the time development the system starting from near the racemic state achieves a homochiral state under grinding. The grinding makes the racemic state unstable and the exponential amplification appears when the system escapes from the racemic state to the homochiral state. The racemic state is the unstable fixed point $(z^{\mathrm{u}},x_{\mathrm{c}}^{\mathrm{u}},y_{\mathrm{c}}^{\mathrm{u}},x_{\mathrm{s}}^{\mathrm{u}},y_{\mathrm{s}}^{\mathrm{u}})$ of Eqs. (1)–(5) or (6)–(10) in the case without chiral impurities. With impurities, the time development of the EE of clusters, $\phi_{\mathrm{c}} = (x_{\mathrm{c}} - y_{\mathrm{c}})/(x_{\mathrm{c}} + y_{\mathrm{c}})$, and that of solids ϕ_{s} for type I impurities are obtained from Eqs. (1)–(5) as

$$\begin{aligned}\dot{\phi}_{\mathrm{c}} &= -\frac{k_{\mathrm{cs}}}{2}(x_{\mathrm{s}}+y_{\mathrm{s}})(1-\phi_{\mathrm{c}}^2)\phi_{\mathrm{s}} + \lambda_{\mathrm{cs}}\frac{x_{\mathrm{s}}+y_{\mathrm{s}}}{x_{\mathrm{c}}+y_{\mathrm{c}}}(\phi_{\mathrm{s}}-\phi_{\mathrm{c}}) \\ &\quad + \frac{1-\alpha_{\mathrm{I}}}{2}k_{1\mathrm{c}}z(1-\phi_{\mathrm{c}}^2) \\ &\quad - \frac{1-\gamma_{\mathrm{I}}}{2}\frac{k_{\mathrm{cs}}}{2}(x_{\mathrm{s}}+y_{\mathrm{s}})(1-\phi_{\mathrm{c}}^2)(1-\phi_{\mathrm{s}}), \qquad (11)\\ \dot{\phi}_{\mathrm{s}} &= \frac{k_{\mathrm{cs}}}{2}(x_{\mathrm{c}}+y_{\mathrm{c}})\phi_{\mathrm{c}}(1-\phi_{\mathrm{s}}^2) + \frac{1-\beta_{\mathrm{I}}}{2}k_{1\mathrm{s}}z(1-\phi_{\mathrm{s}}^2) \\ &\quad + \frac{1-\gamma_{\mathrm{I}}}{2}\frac{k_{\mathrm{cs}}}{2}(x_{\mathrm{c}}+y_{\mathrm{c}})(1-\phi_{\mathrm{c}})(1-\phi_{\mathrm{s}}^2). \qquad (12)\end{aligned}$$

And that for type II impurities are obtained from Eqs. (6)–(10) as

$$\begin{aligned}\dot{\phi}_{\mathrm{c}} =& -\frac{k_{\mathrm{cs}}}{2}(x_{\mathrm{s}}+y_{\mathrm{s}})(1-\phi_{\mathrm{c}}^2)\phi_{\mathrm{s}} + \lambda_{\mathrm{cs}}\frac{x_{\mathrm{s}}+y_{\mathrm{s}}}{x_{\mathrm{c}}+y_{\mathrm{c}}}(\phi_{\mathrm{s}}-\phi_{\mathrm{c}}) + \frac{1-\alpha_{\mathrm{II}}}{2}(k_{1\mathrm{c}}z-\lambda_{1\mathrm{c}})(1-\phi_{\mathrm{c}}^2) \\ & - \frac{1-\gamma_{\mathrm{II}}}{2}\left\{\frac{k_{\mathrm{cs}}}{2}(x_{\mathrm{s}}+y_{\mathrm{s}})(1-\phi_{\mathrm{c}}^2)(1-\phi_{\mathrm{s}}) + \lambda_{\mathrm{cs}}\frac{x_{\mathrm{s}}+y_{\mathrm{s}}}{x_{\mathrm{c}}+y_{\mathrm{c}}}(1+\phi_{\mathrm{c}})(1-\phi_{\mathrm{s}})\right\}, \qquad (13)\end{aligned}$$

$$\dot{\phi}_{\mathrm{s}} = \frac{k_{\mathrm{cs}}}{2}(x_{\mathrm{c}}+y_{\mathrm{c}})\phi_{\mathrm{c}}(1-\phi_{\mathrm{s}}^2) + \frac{1-\beta_{\mathrm{II}}}{2}(k_{1\mathrm{s}}z-\lambda_{1\mathrm{s}})(1-\phi_{\mathrm{s}}^2) + \frac{1-\gamma_{\mathrm{II}}}{2}\left\{\frac{k_{\mathrm{cs}}}{2}(x_{\mathrm{c}}+y_{\mathrm{c}})(1-\phi_{\mathrm{c}})(1-\phi_{\mathrm{s}}^2) - \lambda_{\mathrm{cs}}(1-\phi_{\mathrm{s}}^2)\right\}. \qquad (14)$$

Various previous numerical studies [12,14,18,26,28] suggest that total mass of clusters $x_{\mathrm{c}} + y_{\mathrm{c}}$ and that of solids $x_{\mathrm{s}} + y_{\mathrm{s}}$ stay constant during the amplification of the EE, and we may assume that the total masses are constant. After the linear approximation in ϕ_{c} and ϕ_{s} for Eqs. (11) and (12), we obtain the second derivative of ϕ_{c} on time using $\dot{\phi}_{\mathrm{s}}$. The time development of ϕ_{c} and that of ϕ_{s} with type I impurities are written as

$$\begin{aligned}&\ddot{\phi}_{\mathrm{c}} + \lambda'\dot{\phi}_{\mathrm{c}} + (1-\tilde{\gamma}_{\mathrm{I}})k''\{(1-\tilde{\gamma}_{\mathrm{I}})k' - \lambda'\} \\ &\quad \times \left(\phi_{\mathrm{c}} + \frac{\tilde{\beta}_{\mathrm{I}}k_{1\mathrm{s}}z + \tilde{\gamma}_{\mathrm{I}}k''}{(1-\tilde{\gamma}_{\mathrm{I}})k''}\right) = 0, \qquad (15)\\ &\dot{\phi}_{\mathrm{s}} = (1-\tilde{\gamma}_{\mathrm{I}})k''\phi_{\mathrm{c}} + \tilde{\beta}_{\mathrm{I}}k_{1\mathrm{s}}z + \tilde{\gamma}_{\mathrm{I}}k'', \qquad (16)\end{aligned}$$

where

$$k' = \frac{k_{\mathrm{cs}}}{2}(x_{\mathrm{s}}+y_{\mathrm{s}}), \qquad (17)$$

$$\lambda' = \lambda_{\mathrm{cs}}\frac{x_{\mathrm{s}}+y_{\mathrm{s}}}{x_{\mathrm{c}}+y_{\mathrm{c}}}, \qquad (18)$$

$$k'' = \frac{k_{\mathrm{cs}}}{2}(x_{\mathrm{c}}+y_{\mathrm{c}}), \qquad (19)$$

$$\tilde{\beta}_{\mathrm{I}} = \frac{1-\beta_{\mathrm{I}}}{2}, \qquad (20)$$

$$\tilde{\gamma}_{\mathrm{I}} = \frac{1-\gamma_{\mathrm{I}}}{2}. \qquad (21)$$

And with type II impurities,

$$\begin{aligned}&\ddot{\phi}_{\mathrm{c}} + (1-\tilde{\gamma}_{\mathrm{II}})\lambda'\dot{\phi}_{\mathrm{c}} + (1-\tilde{\gamma}_{\mathrm{II}})^2k''\{k' - \lambda'\} \\ &\quad \times \left(\phi_{\mathrm{c}} + \frac{\tilde{\beta}_{\mathrm{II}}(k_{1\mathrm{s}}z-\lambda_{1\mathrm{s}}) + \tilde{\gamma}_{\mathrm{II}}(k''-\lambda_{\mathrm{cs}})}{(1-\tilde{\gamma}_{\mathrm{II}})k''}\right) = 0, \qquad (22)\\ &\dot{\phi}_{\mathrm{s}} = (1-\tilde{\gamma}_{\mathrm{II}})k''\phi_{\mathrm{c}} + \tilde{\beta}_{\mathrm{II}}(k_{1\mathrm{s}}z-\lambda_{1\mathrm{s}}) + \tilde{\gamma}_{\mathrm{II}}(k''-\lambda_{\mathrm{cs}}), \qquad (23)\end{aligned}$$

where

$$\tilde{\beta}_{\mathrm{II}} = \frac{1-\beta_{\mathrm{II}}}{2}, \qquad (24)$$

$$\tilde{\gamma}_{\mathrm{II}} = \frac{1-\gamma_{\mathrm{II}}}{2}. \qquad (25)$$

We note that $\tilde{\beta}$ and $\tilde{\gamma}$ represent the degree of the asymmetry, that is, $\tilde{\beta} = 0$ when $\beta = 1$ and $\tilde{\beta} = 1/2$ when $\beta = 0$.

In both cases, the change of ϕ_{c} is written in terms of an exponential function with a constant: $(\phi_{\mathrm{c}} - \phi_{\mathrm{c}}^{\mathrm{u}}) \sim e^{\omega t}$, where

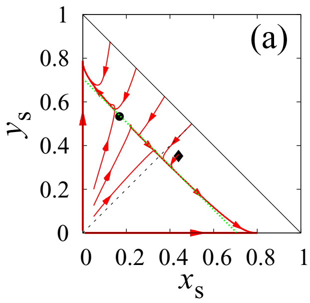

FIG. 3. Projection of mass flow with (a) $(\alpha_{\rm I},\beta_{\rm I},\gamma_{\rm I}) = (1,0.9,1)$ in Eqs. (1)–(5) and (b) $(\alpha_{\rm II},\beta_{\rm II},\gamma_{\rm II}) = (1,0.25,1)$ in Eqs. (6)–(10). Red lines show the trajectory of the system. The black circle represents the unstable fixed point $(x_{\rm s}^{\rm u},y_{\rm s}^{\rm u})$. The green broken line, black solid line, and green dotted line represent $x_{\rm s} = y_{\rm s}$, $x_{\rm s} + y_{\rm s} = 1$, and $x_{\rm s} + y_{\rm s} = x_{\rm s}^{\rm u} + y_{\rm s}^{\rm u}$, respectively. The black diamond represents the starting point in the case of Figs. 2(a) and 2(b), respectively.

ω [Eqs. (26) and (27)] and $\phi_{\rm c}^{\rm u}$ [Eqs. (28) and (29)] are the amplification rate and the unstable fixed point. Since the time development of $\phi_{\rm s}$ is obtained from the first derivative of $\phi_{\rm c}$ [Eqs. (16) and (23)], $\phi_{\rm s}$ is also an exponential function with the same amplification rate ω. This result suggests that the EE amplification is exponential even with impurities. The exponential amplification rates are

$$\omega_{\rm I}^{\pm} = \frac{-\lambda' \pm \sqrt{\lambda'^2 - 4(1-\tilde{\gamma}_{\rm I})k''\{(1-\tilde{\gamma}_{\rm I})k' - \lambda'\}}}{2}, \qquad (26)$$

$$\omega_{\rm II}^{\pm} = \frac{1-\tilde{\gamma}_{\rm II}}{2}\left(-\lambda' \pm \sqrt{\lambda'^2 - 4k''(k'-\lambda')}\right). \qquad (27)$$

The fast relaxation with the rate $\omega^- < 0$ represents the relaxation in the case of $(\phi_{\rm c} - \phi_{\rm c}^{\rm u})(\phi_{\rm s} - \phi_{\rm s}^{\rm u}) < 0$ where $\phi_{\rm c}^{\rm u}$ and $\phi_{\rm s}^{\rm u}$ represent the EE of clusters and that of solids at the unstable fixed point, respectively. The slow relaxation rate ω^+ relating to $(\phi_{\rm c} - \phi_{\rm c}^{\rm u})(\phi_{\rm s} - \phi_{\rm s}^{\rm u}) > 0$ is important for the amplification of the EE. In order to clarify the meanings of the obtained amplification rate ω^+, some trajectories of the mass flow of solids with type I and type II impurities are shown in Figs. 3(a) and 3(b), respectively. The black circle shows the unstable state $(x_{\rm s}^{\rm u},y_{\rm s}^{\rm u})$. The green broken line represents $x_{\rm s} = y_{\rm s}$ $(\phi_{\rm s} = 0)$. One feature of the flow is that the system approaches the line $x_{\rm s} + y_{\rm s} = x_{\rm s}^{\rm u} + y_{\rm s}^{\rm u}$ from most initial conditions. When the system reaches the line $x_{\rm s} + y_{\rm s} = x_{\rm s}^{\rm u} + y_{\rm s}^{\rm u}$, the system escapes from the unstable fixed point along the line to the stable fixed point ($x_{\rm s} = 0$ or $y_{\rm s} = 0$). The relaxation rate ω^+ corresponds to the escape rate from the unstable fixed point. This feature is also observed in the case of the blue dotted line in Figs. 2(a) and 2(b), whose initial condition is shown by the diamond in Figs. 3(a) and 3(b).

Before the interpretation of the linear approximation analysis, we mention an intuitive understanding from the effective mass flow during the EE amplification shown in Fig. 4, which is obtained from a numerical calculation of our model. As chiral solids are ground by glass beads, a large mass flow from the solids to the clusters is realized by a large decay rate $\lambda_{\rm cs}$ and accumulated clusters release a large amount of monomers. The supersaturated monomers solidify, that is, the large mass flow from the monomers to the solids is realized. For type I impurities, small $\alpha_{\rm I}$ and $\gamma_{\rm I}$ lead to the fast dissolution of minority crystals $\rm Y_s$ and small $\beta_{\rm I}$ prevents the crystallization of the solid $\rm Y_s$ from monomers Z (see Fig. 1). All type I impurities work as a reduction factor of the $\rm Y_s$ production and the majority crystals $\rm X_s$ prevail. For type II impurities, when $\alpha_{\rm II}$ and $\gamma_{\rm II}$ are smaller than unity, solids $\rm Y_s$ become difficult to decay and they prevail. When $\beta_{\rm II}$ is smaller than unity, solids $\rm Y_s$ become difficult to grow even in supersaturation and solids $\rm X_s$ grow faster. The suppression of the growth rate with monomers, represented by the parameter $\beta_{\rm II}$, is important for the dominance of the majority of the crystals.

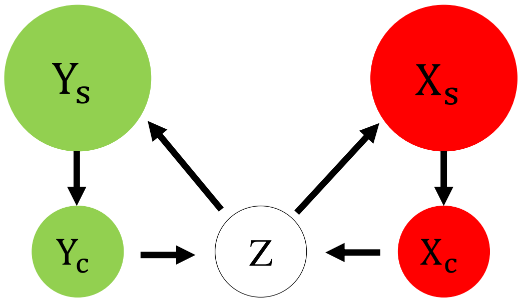

FIG. 4. Effective mass flow during Viedma ripening.

Based on the intuitive understanding of the mass flow, we discuss the effect of the reduction parameters on the amplification of the EE. Although the unstable fixed point depends on the reduction parameters, we assume that the effect of reduction parameters is not significant to the masses $x_{\rm c}^{\rm u} + y_{\rm c}^{\rm u}$ and $x_{\rm s}^{\rm u} + y_{\rm s}^{\rm u}$, which seems valid in the cases we studied. From Eqs. (26) and (27), the EE amplification rate depends only on $\gamma_{\rm I}$ or $\gamma_{\rm II}$ in the viewpoint of the impurity effect. The reduction parameters $\gamma_{\rm I}$ and $\gamma_{\rm II}$ lead to the small amplification rate. It is also important to know how chiral impurities change the sign of $\phi_{\rm s}^{\rm u}$ since the state $\phi_{\rm s}(t = \infty)$ is related with the sign of $\phi_{\rm s}(0) - \phi_{\rm s}^{\rm u}$, where $\phi_{\rm s}(0) \approx 0$ is the initial EE. We discuss $\phi_{\rm s}(\infty)$ using $\phi_{\rm c}^{\rm u}$ because $\phi_{\rm s}(t)$ is proportional to $[\phi_{\rm c}(0) - \phi_{\rm c}^{\rm u}]e^{\omega^+ t}$ when the time change of $\phi_{\rm c}(t)$ is written as $[\phi_{\rm c}(0) - \phi_{\rm c}^{u}]e^{\omega^+ t}$ [see Eqs. (16) and (23)].

From Eq. (15), the unstable fixed point of clusters $\phi_{\rm c}^{u}$ for type I impurities is obtained as

$$\phi_{\rm c}^{\rm u} = -\frac{\tilde{\beta}_{\rm I}k_{1{\rm s}}z + \tilde{\gamma}_{\rm I}k''}{(1-\tilde{\gamma}_{\rm I})k''}. \qquad (28)$$

Since $\beta_{\rm I}$ and $\gamma_{\rm I}$ are positive, $\phi_{\rm c}^{\rm u}$ becomes negative, and the final state is predicted as $\phi_{\rm s}(\infty) = 1$ when the initial state is the racemic state [$\phi_{\rm s}(0) \approx 0$]. The effect of $\alpha_{\rm I}$ on $\phi_{\rm c}^{\rm u}$ is not trivial. From Eq. (11), $\alpha_{\rm I} < 1$ increases $\dot{\phi}_{\rm c}$ at the racemic state and leads to $\phi_{\rm s}^{\rm u} < 0$.

From Eq. (22), the unstable fixed point of clusters for type II is

$$\phi_{\rm c}^{\rm u} = -\frac{\tilde{\beta}_{\rm II}(k_{1{\rm s}}z - \lambda_{1{\rm s}}) + \tilde{\gamma}_{\rm II}(k'' - \lambda_{\rm cs})}{(1-\tilde{\gamma}_{\rm II})k''}. \qquad (29)$$

The reduction parameter $\beta_{\rm II}$ leads to the negative sign of $\phi_{\rm c}^{\rm u}$ since the effective mass flow from monomers to the solids is positive ($k_{1{\rm s}}z - \lambda_{1{\rm s}} > 0$) during the amplification of the EE. $\gamma_{\rm II}$ leads to the positive sign of $\phi_{\rm c}^{\rm u}$ because of a large $\lambda_{\rm cs}$.

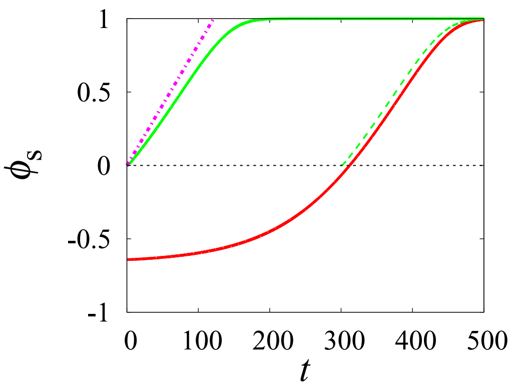

FIG. 5. Time change of the EE from $\phi_s = -0.64$ [red (black) solid line] and from the racemic state $\phi_s = 0$ [green (gray) solid line]. The green (gray) broken line shows the green (gray) solid line shifted to $t + 300$. Magenta (gray) dash-dotted line shows the estimated line from Eq. (30). The parameters are the same in the case of Fig. 2(b) (type II) and the unstable fixed point is $\phi_s^u = -0.66$.

The effect of $\alpha_{\rm II}$ on ϕ_c^u is not trivial as in the case of the type I impurities. From Eq. (13), $\alpha_{\rm II} < 1$ leads to the negative sign of $\dot{\phi}_c$ at the racemic state since the mass flow from the monomers to the clusters is negative ($k_{1c}z - \lambda_{1c} < 0$) during the EE amplification and $\phi_s^u > 0$ is probably realized.

The above interpretations are consistent with the numerical result shown in Fig. 2. With the parameters in Fig. 2, the values of ϕ_c^u with $\beta_{\rm I}$ and $\gamma_{\rm I}$ are predicted as -0.07 and -0.05, respectively. As the amplification rate with $\gamma_{\rm I}$ becomes smaller than that with $\beta_{\rm I}$ [see Eqs. (26) and (27)], the saturation time, when ϕ_s is achieved to unity, with $\gamma_{\rm I}$ is larger than that with $\beta_{\rm I}$. The reduction parameter $\beta_{\rm II}$ produces a similar effect as $\beta_{\rm I}$. $\alpha_{\rm II}$ and $\gamma_{\rm II}$ lead to the opposite sign of ϕ_s compared to the case with $\alpha_{\rm I}$ and $\gamma_{\rm I}$. The difference of the impurity effect on type I and type II comes from the different direct effect of the impurities, i.e., the reduction of the growth rate or that of the mass flow between components.

We now consider the linear amplification of the EE observed experimentally in Ref. [24].

Figure 5 shows the time change of the EE with $(\alpha_{\rm II},\beta_{\rm II},\gamma_{\rm II}) = (1,0.25,1)$ for various initial conditions. Starting from $\phi_s = -0.64$ [red (black) solid line], which is close to the unstable fixed point $\phi_s^u = -0.66$, the exponential amplification is observed. On the other hand, starting from the racemic state $\phi_s = 0$, where the system is far from the unstable fixed point, the linear amplification is seen [green (gray) solid line]. The change of the EE is similar to the part of the exponential amplification (the shifted EE line is shown by the green broken line in Fig. 5). The apparent linear amplification rate can be estimated by

$$\omega^{\mathrm{l}} = \left.\frac{d\phi_s(t)}{dt}\right|_{\phi_s=0} = -\omega^{+}\phi_s^u > 0, \qquad (30)$$

which comes from $\phi_s(t) - \phi_s^u = [\phi_s(0) - \phi_s^u]\exp(\omega^+ t)$ with Eq. (27). As shown in Fig. 5, the estimation by Eq. (30) [magenta (gray) dash-dotted line] is in reasonable agreement with the numerical result [green (gray) solid line]. The apparent linear amplification of the EE from the racemic state suggests that mathematically the starting point of the exponential amplification is shifted from the racemic state and hidden.

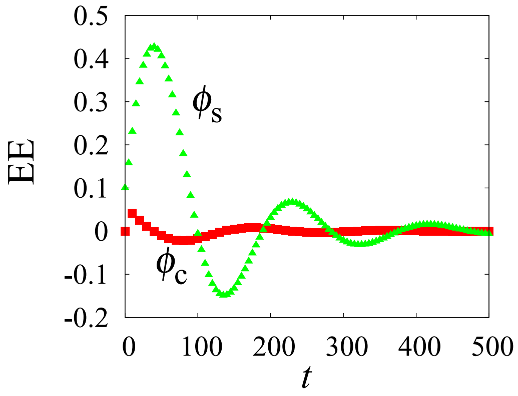

FIG. 6. Time dependence of ϕ_c [red (black) square] and ϕ_s [green (gray) triangle] without impurities from the direct numerical calculation. Parameters are $k_{1c} = 0.1$, $k_{1s} = k_{cs} = 1$, $\lambda_{1c} = 0.001$, $\lambda_{1s} = 0.1$, $\lambda_{cs} = 0.4$.

Finally, we comment on the amplification rate Eqs. (26) and (27). Firstly, $\lambda' > k'$ is required for the chirality conversion in the case of type II impurities [Eq. (27)]. In the case of type I impurities [Eq. (26)], the condition is looser. The EE amplification is realized by the grinding because the grinding provides a large $\lambda_{cs} \sim \lambda'$. The reduction of the growth rate between clusters and solids $k_{cs} \sim k'$ also works in the same sense.

Secondly, we note that the relaxation rate to the unstable state can have an imaginary part, even without impurities, when $\lambda'^2 - 4k''(k' - \lambda') < 0$. The EE may relax toward the unstable state with oscillation and it is confirmed by the numerical calculation with the parameters $(k_{1c},k_{1s},k_{cs},\lambda_{1c},\lambda_{1s},\lambda_{cs}) = (0.1,1,1,0.001,0.1,0.4)$ as shown in Fig. 6. Starting from the initial condition $\phi_s = 0.1$, which is the same as in the case of Fig. 2, the EE of solids becomes more than 0.4 at $t \simeq 50$, and a clear oscillatory relaxation is seen. The EE of clusters ϕ_c also slightly oscillates with a different phase.

IV. SUMMARY

We studied the effect of chiral impurities on the EE amplification in a grinding system using the rate equation model. We considered the two types of impurities: type I changes the equilibrium balance of each component, and type II changes the growth and dissolution rate with the same ratio. In our numerical study, we found the following: Type I impurities that hinder the incorporation processes of the minority species accelerate the EE amplification. Type II impurities accelerate the EE amplification when the chiral impurities suppress the reaction rates between monomers and solids of the minority. When the type II impurities suppress the reaction rates between monomers and clusters or between clusters and solids, the EE changes the sign and the minority crystals prevail. The effect of impurities depends on how impurities change the mass flow shown in Fig. 4. When the impurities ($\alpha_{\rm I}$ and $\gamma_{\rm I}$) make the minority solids easy to dissolve or the impurities ($\beta_{\rm I}$ and $\beta_{\rm II}$) make them difficult to grow, the EE amplification is accelerated and the minority crystals diminish faster. When the impurities (α_{II} and γ_{II}) make the minority solids difficult to dissolve, the minority crystals prevail. From the analysis of the time development of the EE, we found that the EE is amplified exponentially with time from the unstable fixed point even when the linear amplification from the racemic state is seen. Chiral impurities shift the unstable fixed point of the exponential amplification from the racemic state.

The case of type II impurities with $\alpha_{\mathrm{II}} = 0$ and $\beta_{\mathrm{II}} = \gamma_{\mathrm{II}}$ corresponds to the reaction model in the previous work [24]. The linear change of components is also observed in our study and our numerical results are consistent with theirs. Our conclusion is that the observed linear amplification in the experiment [24] is interpreted as a part of the exponential amplification. Even if the EE is amplified linearly from the racemic state, the exponential amplification will be seen when the system starts from near the unstable fixed point.

As a result of the linear analysis of the simple rate equation model, we found the possibility of the oscillatory relaxation of the EE. Although this oscillatory relaxation is confirmed using the direct numerical calculation of the simple rate equation, it is not certain that the oscillation really occurs since the crystal size distribution is not taken into account.

ACKNOWLEDGMENT

This work is supported by JSPS KAKENHI Grant No. JP15K05127.

---

[1] D. K. Kondepudi, R. Kaufman, and N. Singh, Science **250**, 975 (1990).

[2] For a review, see D. K. Kondepudi and K. Asakura, Acc. Chem. Res. **34**, 946 (2001).

[3] For a review, see Y. Saito and H. Hyuga, Rev. Mod. Phys. **85**, 603 (2013).

[4] J. M. McBride and R. I. Carter, Angew. Chem., Int. Ed. Engl. **30**, 293 (1991).

[5] B. Martin, A. Tharrington, and X-l. Wu, Phys. Rev. Lett. **77**, 2826 (1996).

[6] R.-U. Qian and G. D. Botsaris, Chem. Eng. Sci. **53**, 1745 (1998).

[7] T. Buhse, D. Durand, D. Kondepudi, J. Laudadio, and S. Spilker, Phys. Rev. Lett. **84**, 4405 (2000).

[8] Y. Song, W. Chen, and X. Chen, Cryst. Growth Des. **8**, 1448 (2008).

[9] C. Viedma, Phys. Rev. Lett. **94**, 065504 (2005).

[10] W. L. Noorduin, T. Izumi, A. Millemaggi, M. Leeman, H. Meekes, W. J. P. van Enckevort, R. M. Kellogg, B. Kaptein, E. Vlieg, and D. G. Blackmond, J. Am. Chem. Soc. **130**, 1158 (2008).

[11] For reviews, see W. L. Noorduin, E. Vlieg, R. M. Kellogg, and B. Kaptein, Angew. Chem., Int. Ed. **48**, 9600 (2009); L.-C. Sögütoglu, R. R. E. Steendam, H. Meekes, E. Vlieg and F. P. J. T. Rutjes, Chem. Soc. Rev. **44**, 6723 (2015).

[12] M. Uwaha, J. Phys. Soc. Jpn. **73**, 2601 (2004).

[13] J. A. D Wattis and P. V. Coveney, Org. Life Evol. Biosph. **35**, 243 (2005).

[14] M. Uwaha, J. Phys. Soc. Jpn. **77**, 083802 (2008).

[15] M. Uwaha and H. Katsuno, J. Phys. Soc. Jpn. **78**, 023601 (2009).

[16] H. Katsuno and M. Uwaha, J. Cryst. Growth **311**, 4265 (2009).

[17] W. L. Noorduin, W. J. P. van Enckevort, H. Meekes, B. Kaptein, R. M. Kellogg, J. C. Tully, J. M. McBride, and E. Vlieg, Angew. Chem., Int. Ed. **49**, 8435 (2010).

[18] J. A. D. Wattis, Orig. Life Evol. Biosph. **41**, 133 (2011).

[19] M. Iggland and M. Mazzotti, Cryst. Growth Des. **11**, 4611 (2011).

[20] M. Iggland and M. Mazzotti, CrystEngComm **15**, 2319 (2013).

[21] C. Blanco, J. Crusats, Z. El-Hachemi, A. Moyano, S. Veintemillas-Verdaguer, D. Hochberg, and J. M. Ribó, ChemPhysChem **14**, 3982 (2013).

[22] F. Ricci, F. H. Stillinger, and P. G. Debenedetti, J. Chem. Phys. **139**, 174503 (2013).

[23] C. Blanco, J. M. Ribó, and D. Hochberg, Phys. Rev. E **91**, 022801 (2015).

[24] R. R. E. Steendam, J. Dickhout, W. J. P. van Enckevort, H. Meekes, J. Raap, F. P. J. Tutjes, and E. Vlieg, Cryst. Growth Des. **15**, 1975 (2015).

[25] Y. Saito and H. Hyuga, J. Phys. Soc. Jpn. **77**, 113001 (2008).

[26] Y. Saito and H. Hyuga, J. Phys. Soc. Jpn. **79**, 083002 (2010).

[27] Y. Saito and H. Hyuga, J. Cryst. Growth **318**, 93 (2011).

[28] Y. Saito and H. Hyuga, J. Phys. Soc. Jpn. **73**, 33 (2004).

[29] W. L. Noorduin, P. van der Asdonk, H. Meekes, W. J. P. van Enckevort, B. Kaptein, M. Leeman, R. M. Kellogg, and E. Vlieg, Angew. Chem., Int. Ed. **48**, 3278 (2009).

[30] H. Katsuno and M. Uwaha, Phys. Rev. E **86**, 051608 (2012).

[31] The values of parameters with grinding are not directly related to the values that realize the equilibrium masses. Since the circulating mass flow during Viedma ripening (Fig. 4) seems essential [14,17], we choose the parameter values rather arbitrarily to realize the circulating flow.